Jurnal Kejuruteraan 36(3) 2024: 1199–1205
https://doi.org/10.17576/jkukm-2024-36(3)-29

Microhardness and Microstructure of Aluminium Alloy 5052 by High-Pressure Torsion Process and Subsequent Annealing

Ahmad Muhammad Aziz, Intan Fadhlina Mohamed [a*], Mohd Zaidi Omar[a], Zainuddin Sajuri[a], Norinsan Kamil Othman[b], Mohammad Azlan Aripin[a,c], Nor Kamaliana Khamis[a], & Hawa Hishamuddin[a]

[a]*Department of Mechanical and Manufacturing Engineering, Faculty of Engineering and Built Environment, Universiti Kebangsaan Malaysia, 43600 Bangi, Selangor, Malaysia,*

[b]*Department of Applied Physics, Faculty of Science and Technology, Universiti Kebangsaan Malaysia, 43600 Bangi, Selangor, Malaysia,*

[c]*Department of Mechanical Engineering, Faculty of Engineering, City University, 46100, Petaling Jaya, Selangor, Malaysia*

[*]*Corresponding author: intanfadhlina@ukm.edu.my*

Received 5 January 2023, Received in revised form 16 February 2024
Accepted 2 March 2024, Available online 30 May 2024

ABSTRACT

The grain refinement by high-pressure torsion (HPT) process and high-temperature stability have been studied in a commercial non-heat-treated aluminium alloy, 5052. The HPT process was conducted on 10 mm disks of the alloys at room temperature with an applied pressure of 6 GPa for 5 and 10 turns with a rotation speed of 1 rpm. The HPT processing leads to microstructural refinement with an average grain size of ~188 nm and ~156 nm for 5 turns and 10 turns with an increased value of dislocation density. The Vickers microhardness test was performed at 100 gf for a duration of 15 s. It was found that the hardness increased from the onset of straining and saturated at approximately 165 Hv after processing at both 5 and 10 turns. The samples were then annealed at high temperatures. The study demonstrated that annealing at 200 °C for 1 h reduced the hardness by 30% in both samples and enlarged the gain sizes to 226 nm. The results indicated that the rate of hardness decrease is faster in 10 turns compared with 5 turns thus explaining the higher kinetic annihilation phenomenon observed in higher straining in 10 turns due to the higher stored energy in the grains.

Keywords: AA5052; Non-heat-treated aluminium alloy; Severe plastic deformation; Ultrafine-grained material

INTRODUCTION

A severe plastic deformation (SPD) process can increase a material's mechanical properties by up to 300 % (Abd El Aal & Kim 2014). Many studies reported the behaviour of the material after deformation, as the SPD process is capable of producing materials with remarkable mechanical properties (Cheeranan et al. 2020; Mohamed et al. 2016). The significant improvement in mechanical properties attained through the SPD process unveils numerous possibilities for applications in various industries, including aerospace, automotive, and manufacturing. These sectors, which prioritize lightweight and high-strength materials in the industries can greatly benefit from the advancement of this process (Mamgain et al. 2023). A wide range of materials, including metals (Deng et al. 2020), ceramics (Edalati et al. 2019), glass (Ebner et al. 2018), and rare earth (Sun et al. 2018) are used in research on the SPD process. The primary benefit of the SPD process is the deformation that can occur without changing the material's original shape.

The SPD process such as accumulative rolling bonding (ARB) (Chen et al. 2020), equal channel angular pressing (ECAP) (Kalsar et al. 2020), and high-pressure torsion (HPT) (Machado et al. 2023), is successful in deforming a material when it is in its bulk state and produces

outstanding mechanical properties. However, the HPT process is the most well-known among the SPD processes because of its ability to generate significant strain during deformation and lead to astonishing performance (Gebril et al. 2018; Komatsu et al. 2023; Orlov et al. 2012).

Although the SPD process demonstrated exceptional mechanical properties, exposure to high temperatures can adversely affect the performance of SPD materials, causing the structure of the grains to become unstable (Aziz et al. 2024; Zhang et al. 2020). Wang et al. (2018) have studied the effect of high-temperature stability of commercial AA5052 with the addition of erbium (Er). The addition of Er increased the hardness of AA5052 to 95 Hv and sustained the hardness while annealing up to 320 °C. Thus, it is crucial to comprehend the high-temperature stability when the AA5052 with enhanced strengthening by SPD is exposed to high-temperature.

This investigation aims to explore microstructure and microhardness changes when AA5052 is exposed to high temperatures. In this study, we assess the ability of the HPT process to produce ultrafine grain. The response of the AA5052 alloy to the annealing process is observed, and the effect of straining on the annealing process is examined.

METHODOLOGY

Samples of aluminium alloy 5052 was received in a form of sheet with thickness of 1 mm. The chemical composition of the alloy used in this study is shown in Table 1. The sheet material was cut using an electric discharge machine (EDM) into disks with diameter of 10 mm. Then, the alloy was solution-treated at 520 °C for 4 h and cooled at room temperature (R.T.) before HPT processing. Samples with 10 mm in diameter and 1 mm thickness were processed under an applied pressure of 6 GPa for number of turns *(N)* 5 and 10 at a rotation speed of 1 rpm at RT. X-ray diffraction (XRD) analysis with Cu Kα radiation having a wavelength, λ, 0.15418 nm was carried out using a 3 mm disk with diameter as shown in Figure 1.The disk was polished to a mirror-like surface and the Vickers microhardness was measured at 8 different radial directions with an applied load of 100 g for 15 s, as illustrated in Figure 1.

The microstructure was observed by using Transmission electron microscopy (TEM) analysis at an accelerating voltage of 200 kV after the HPT processing. Selected area electron diffraction (SAED) patterns were taken around regions having diameter of 6.3 µm. A 3 mm disk was extracted at the edge of the sample as shown in Figure 1. The sample was grounded until 0.12 mm thickness and thinned using a twin-jet electropolishing using 20%NHO_3 and 80%CH_3OH solution at temperature of -13 °C with an applied voltage of 12 V.

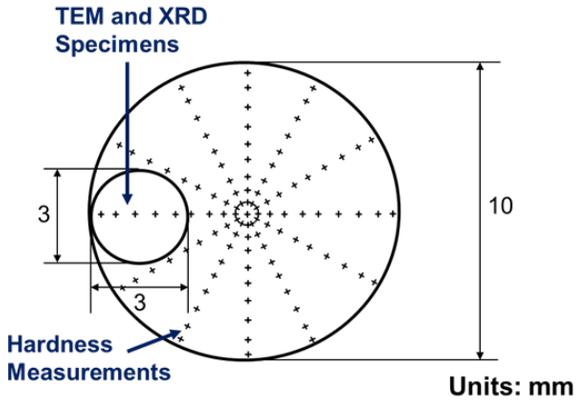

FIGURE 1. Schematic diagram of the HPT disk and locations for hardness measurements, XRD and TEM

RESULTS AND DISCUSSION

Figure 2 illustrates the Vickers microhardness against the distance from the center of the disk to the edge of the disk for the HPT-processed sample of $N = 5$ and 10.

TABLE 1. Chemical composition of AA5052 aluminium alloy (% mass)

Mg	Si	Fe	Cr	Mn	Cu	Al
2.0	0.68	0.31	0.21	0.07	0.02	Bal.

The result shows that the hardness increased from the center of the disk to the edge of the disk regardless of the sample states. The hardness finally saturates at approximately 162 Hv as it approaches the edge of the sample. The hardness of both $N = 5$ and 10 increased above the hardness of the solid solution sample by ~180%. This behaviour is reported earlier by a few researchers (Kong et al. 2020; Mohamed et al. 2017).

However, the hardness for $N = 5$ and 10 decreased to ~ 120 Hv after annealing at 200 °C as in Figure 2. The hardness of the annealed samples decreased by ~ 25% compared to the as-HPT samples.

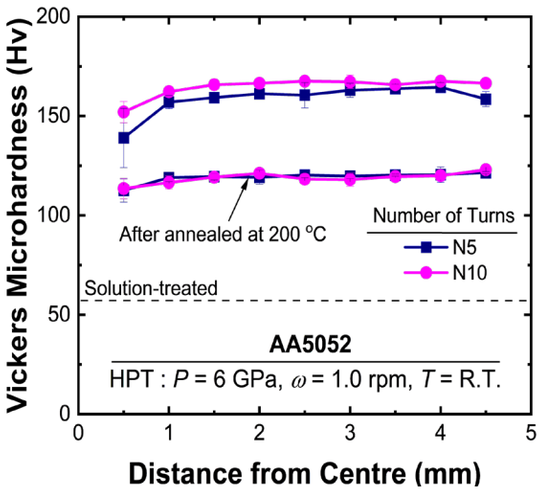

FIGURE 2. Microhardness after the HPT process and subsequent annealing for $N = 5$ and 10

Figure 3 shows the XRD profiles of the HPT samples for $N = 5$ and 10. The comparison of the measured full width at half maximum (FWHM) for solution-treated, $N = 5$ and 10 shows evidence of peak broadening of the XRD profiles. Thus, it confirms the formation of smaller grain sizes by the HPT process. Using the measured FWHM, the Williamson-Hall equation was employed to obtain the dislocation density. Figure 4 shows the dislocation densities and lattice strain plotting for $N = 5$ and 10. The dislocation density calculated for $N = 10$ is 4.9×10^{14} m^{-2}. This value is slightly greater than that of the $N = 5$, which is 4.8×10^{14} m^{-2}. The same trend is observed in the lattice strain of $N = 5$ and 10. This result is consistent with Equation 1 explaining that a greater lattice strain is caused by the increasing number of turns. Increasing the number of turns leads to imposing more straining, ε_{eq} where, N = number of turns, r = radius of the sample and h = thickness of the sample.

$$\varepsilon_{eq} = \frac{2\pi N r}{h\sqrt{3}} \quad (1)$$

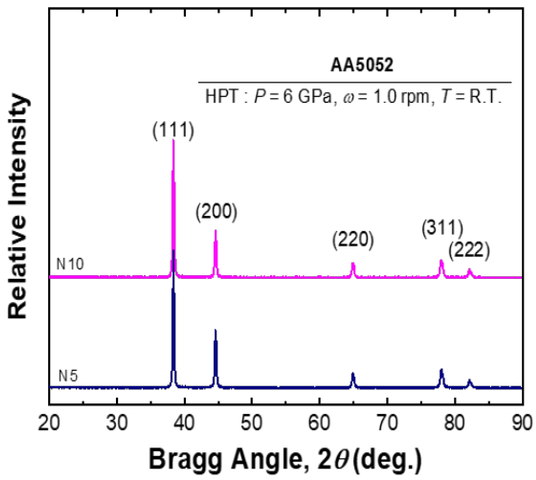

FIGURE 3. XRD profiles of the HPT samples for $N = 5$ and 10

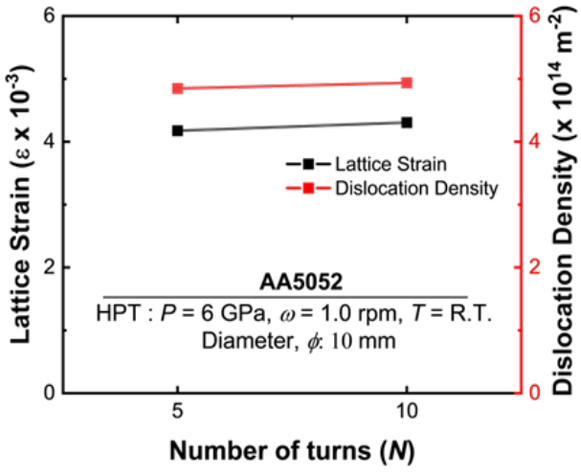

FIGURE 4. Lattice strain and dislocation density of the HPT samples at 5 and 10 turns

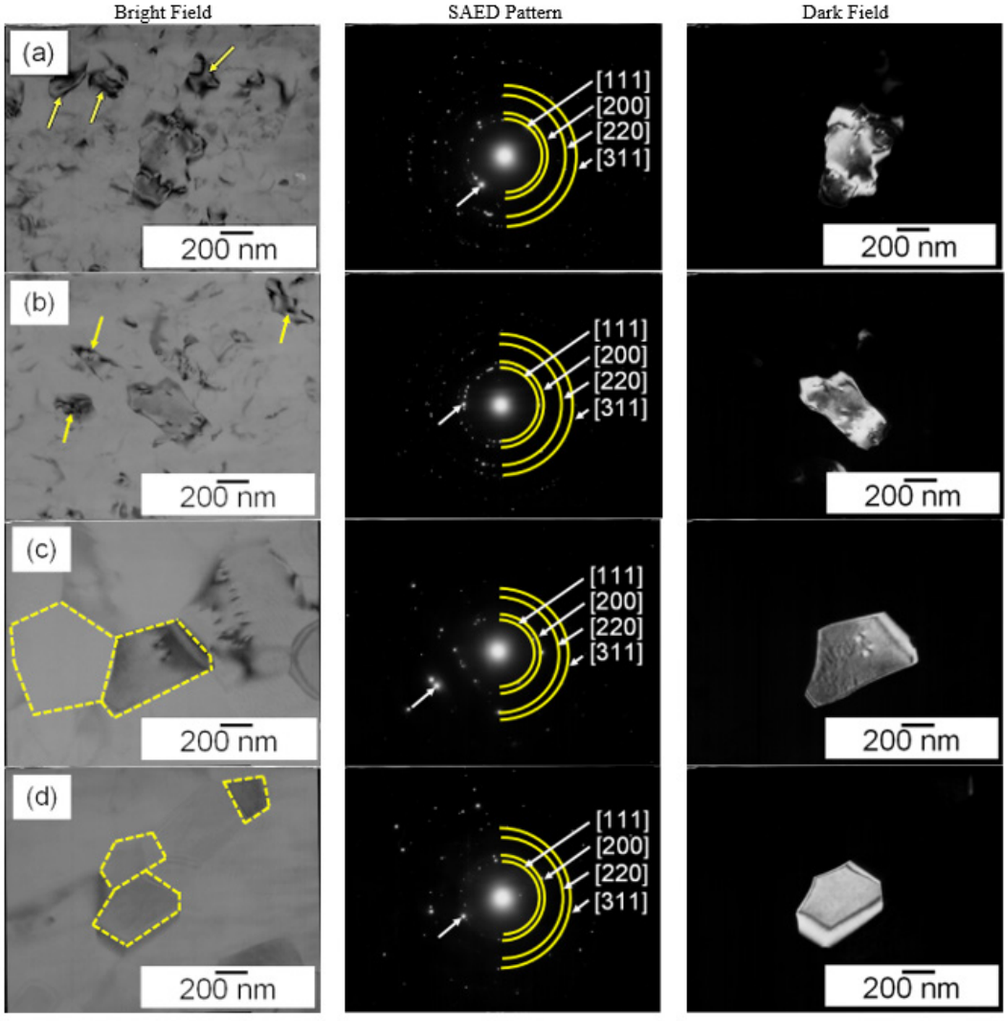

FIGURE 5. TEM micrograph for (a) N = 5 R.T., (b) N =10 R.T., (c) N = 5 200 °C and (d) N = 10 200 °C

Figure 5 shows dark-field, bright-field, and SAED patterns after HPT and annealing processing. Figures 5(a) and 5(b) show the accumulation of the dislocation that occurred in the microstructures of $N = 5$ and 10, as indicated by the yellow arrows.

Besides that, inspection reveals that the SAED patterns exhibit ring-type forms, indicating that the microstructures consist of small grains with high-angle grain boundaries, where the grain size is well in the ultra-fine levels as ~188 ± 37 nm for $N = 5$ and ~156 ± 41 nm for $N = 10$ as in Figure 6. This observation is also reported by Lee et al. (2015) using other SPD techniques. However, when the sample is annealed at 200 °C, the structure of grains becomes more equiaxed as indicated by yellow dotted lines in Figures 5(c) and 5(d). The grain boundaries appear straight and the grains are almost free of dislocations. The grain sizes of the HPT samples for $N = 5$ and 10 enlarged to 245 ± 65 nm and 226 ± 58 nm, respectively as in Figure 6.

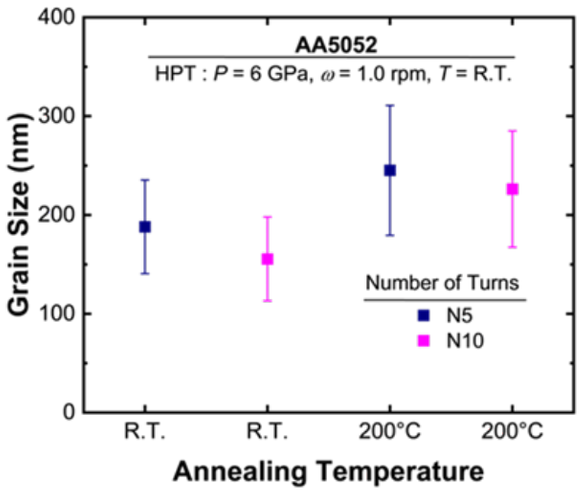

FIGURE 6. Grain size of the HPT processed sample and subsequent annealing of the HPT sample

This situation is also reported by Markushev & Murashkin (2004). The growth of the grain size indicates that the HPT samples exhibit a heat response when subjected to high temperatures. This situation is also mentioned by Summers et al. (2014).

The samples annealed at 200 °C soften due to annihilation of dislocation thus leading to grain growth. The phenomena of recrystallization and grain growth in response to the softening effect after annealing ware mentioned by Krasilnikov et al. (2005).

Moreover, the HPT sample at $N = 10$ exhibited a 10% greater reduction in hardness compared to $N = 5$ after annealing at 200 °C. This occurrence is referred to as a higher rate of kinetic annihilation, observed in a higher straining sample $N = 10$. Kinetic annihilation during the annealing process is attributed to various factors such as the amount of strain that leads to the accumulation of stored energy (Bourezg et al. 2019; Dhal et al. 2017).

The amount of accumulated stored energy in the high-strain, $N = 10$ further influences the kinetic annihilation during the annealing process. Consequently, the rate of kinetic annihilation is higher at $N = 10$ due to this reason. The accumulation of dislocation inside the grain, caused by strain, led to materials retaining significant energy, rendering them sensitive to exposure to high temperatures. Therefore, upon exposure to high temperatures, the structure becomes unstable and leads to recovery and recrystallization processes. It is noted that this behaviour was observed in aluminium alloys by a few researchers in the earlier findings (Farè et al. 2011, Wang et al. 2018).

CONCLUSION

1. The hardness is increased by approximately 180 % through the HPT process.
2. The grain size is reduced to ~156 nm.
3. Post-annealing of the HPT-processed samples led to a decrease in the hardness by ~25 %.
4. The grain size of the annealed sample is increased up to ~226 nm. This indicates that the grain structure is thermally unstable at temperature 200 °C.
5. The higher strain sample at $N = 10$ experienced a greater reduction in hardness compared to $N = 5$. This is attributed to the kinetic annihilation phenomenon during the annealing process.

ACKNOWLEDGEMENT

The authors would like to thank Universiti Kebangsaan Malaysia for their financial support under GUP-2018-150. The authors also gratefully acknowledge the Magnesium Research Center, Kumamoto University, Horita Lab, Kyushu University, and Nagano Forging Co. LTD for supporting via international collaboration research program.

DECLARATION OF COMPETING INTEREST

None

REFERENCES

Aziz, A.M., Mohamed, I.F., Horita, Z., Omar, M.Z., Sajuri, Z., Othman, N.K., Syarif, J., Gebril, M.A., Ostovan, F., Lee, S., Matsuda, K., Yumoto, M., Takizawa, Y. & Hashim Al-Ameri, A.A. 2024. Strengthening of A5052 aluminum alloy by high-pressure sliding process. *Journal of Materials Science* 59: 5754-5770

Bourezg, Y.I., Azzeddine, H., Abib, K., Huang, Y., Bradai, D. & Langdon, T.G. 2019. Recrystallization in an Mg-Nd alloy processed by high-pressure torsion: A calorimetric analysis. *Journal of Materials Research and Technology* 9(3): 3047–3054.

Cheeranan, K.N., Mohamed, I.F., Lamin, F., Wan , Zamri, W.F.H., Omar, M.Z. & Horita, Z. 2020. The Evolvement of Mechanical Properties and Microstructure of Commercial Aluminium Alloy 6061 via High-Pressure Torsion. *Jurnal Kejuruteraan* 32(3): 531-538.

Chen, X., Xia, D., Zhang, J., Huang, G., Liu, K., Tang, A., Jiang, B. & Pan, F. 2020. Ultrafine-grained Al–Zn–Mg–Cu alloy processed via cross accumulative extrusion bonding and subsequent aging: Microstructure and mechanical properties. *Journal of Alloys and Compounds* 846: 156306.

Deng, G., Bhattacharjee, T., Chong, Y., Zheng, R., Bai, Y., Shibata, A. & Tsuji, N. 2020. Influence of Fe addition in CP titanium on phase transformation, microstructure and mechanical properties during high pressure torsion. *Journal of Alloys and Compounds* 822: 153604.

Dhal, A., Panigrahi, S.K. & Shunmugam, M.S. 2017. Insight into the microstructural evolution during cryo-severe plastic deformation and post-deformation annealing of aluminium and its alloys. *Journal of Alloys and Compounds* 726: 1205–1219.

Ebner, C., Escher, B., Gammer, C., Eckert, J., Pauly, S. & Rentenberger, C. 2018. Structural and mechanical characterization of heterogeneities in a CuZr-based bulk metallic glass processed by high pressure torsion. *Acta Materialia* 160: 147–157.

Edalati, K., Fujita, I., Sauvage, X., Arita, M. & Horita, Z. 2019. Microstructure and phase transformations of silica glass and vanadium oxide by severe plastic deformation via high-pressure torsion straining. *Journal of Alloys and Compounds* 779: 394–398.

Jamhari, F.I., Foudzi, F.M., Buhairi, M.A., Sulong, A.B., Mohd Radzuan, N.A., Muhamad, N., Mohamed, I.F., Jamadon, N.H. & Tan, K.S. 2023. Influence of heat treatment parameters on microstructure and mechanical performance of titanium alloy in LPBF: A brief review. *Journal of Materials Research and Technology* 24:4091-4110.

Mohamed, I.F., Lee, S., Edalati, K., Horita, Z., Abdullah, S., Omar, M.Z. & Wan Zamri, W.F.H. 2016. Grain refinement and microstructrue evolution in aluminium A2618 alloy by high-pressure torsion. *Jurnal Teknologi* 78(69): 149-152.

Mohamed, I.F., Masuda, T., Lee, S., Edalati, K., Horita, Z., Hirosawa, S., Matsuda, K., Terada, D. & Omar, M.Z. 2017. Strengthening of A2024 alloy by high-pressure torsion and subsequent aging. *Materials Science and Engineering A* 704: 112-118.

Kalsar, R., Yadav, D., Sharma, A., Brokmeier, H.G., May, J., Höppel, H.W., Skrotzki, W. & Suwas, S. 2020. Effect of Mg content on microstructure, texture and strength of severely equal channel angular pressed aluminium-magnesium alloys. *Materials Science and Engineering A* 797: 140088.

Komatsu, T., Masuda, T., Tang, Y., Mohamed, I.F., Yumoto, M., Takizawa, Y. & Horita, Z. 2023. Production of ultrafine-grained aluminium alloys in upsized sheets using process of incremental feeding high-pressure sliding (IF-HPS). *Materials Transactions* 64(2): 436-442

Krasilnikov, N., Lojkowski, W., Pakiela, Z. & Valiev, R. 2005. Tensile strength and ductility of ultra-fine-grained nickel processed by severe plastic deformation. *Materials Science and Engineering A* 397(1–2): 330–337.

Gebril, M.A., Omar, M.Z., Mohamed, I.F., Othman, N.K. & Abdelgnei, M.A.H. 2018. Corrosion improvementand microstructure evaluation of SEM-solid A356 alloy by ECAP process. Journal of Physics: Conference Series 1082: 012110.

Machado, D.C., Alves Flausino, P.C., Huang, Y., Cetlin, P.R., Langdon, T.G. & Pereira, P.H.R. 2023. Influence of processing temperature on microhardness evolution, microstructure and superplastic behaviour in an Al–Mg alloy processed by high-pressure torsion. *Journal of Materials Research and Technology* 24: 2850–2867.

Mamgain, A., Pratap Singh, A. & Singh, V. 2023. Welding investigation on AA6063-T6 aluminium alloy during friction stir welding process. *Jurnal Kejuruteraan* 35(2): 411–419.

Markushev, M.V. & Murashkin, M.Y. 2004. Structure and mechanical properties of commercial Al–Mg 1560 alloy after equal-channel angular extrusion and annealing. *Materials Science and Engineering A* 367: 234–242.

Abd El Aal, M.I. & Kim, H.S. 2014. Wear properties of high pressure torsion processed ultrafine grained Al7%Si alloy. Materials and Design 53: 373-382

Orlov, D., Todaka, Y., Umemoto, M., Beygelzimer, Y. & Tsuji, N. 2012. Comparative analysis of plastic flow and grain refinement in pure aluminium subjected to simple shear-based severe plastic deformation processing. *Materials Transactions* 53(1): 17–25.

Summers, P.T., Case, S.W. & Lattimer, B.Y. 2014. Residual mechanical properties of aluminium alloys AA5083-H116 and AA6061-T651 after fire. *Engineering Structures* 76: 49–61.

Wang Jinlian, Xu Jun & Pan Feng. 2018. Effect of annealing on microstructure and properties of Er modified 5052 alloy. *Results in Physics* 10: 476-480.

Sun, W.T., Qiao, X.G., Zheng, M.Y., He, Y., Hu, N., Xu, C., Gao, N. & Starink, M.J. 2018. Exceptional grain refinement in a Mg alloy during high pressure torsion due to rare earth containing nanosized precipitates. *Materials Science and Engineering A* 728: 115-123.

Kong, Y., Pu, Q., Jia, Z., Liu, M., Roven, H.J., Jia, J. & Liu, Q. 2020. Microstructure and property evolution of Al-0.4Fe-0.15Zr-0.25Er alloy processed by high pressure torsion. J*ournal of Alloys and Compounds* 824: 153949

Zhang, X., Linke Huang, Zhang, Chen, B., Yuzeng Chen & Liu, F. 2020. Microstructural evolution and strengthening mechanism of an Al–Si–Mg alloy processed by high-pressure torsion with different heat treatments. *Materials Science and Engineering: A* 794: 139932.